Magnet strength measurement in circular accelerators from beam position monitor data

A. Franchi, R. Tomás, and F. Schmidt
CERN, Geneva, Switzerland
(Received 21 March 2007; published 9 July 2007)

Recent measurements of resonance terms suggested the extension of the existing technique to measure magnet strengths from turn-by-turn beam position monitor data. This article describes the algorithm to infer the magnet strength from the variation along the ring of the resonance terms and reports on the first measurement. Both the algorithm and the software written for the analysis of the data can be particularly useful in the commissioning period of an accelerator in order to find magnets with wrong strengths or polarities as well as magnets with large magnetic errors.

DOI: 10.1103/PhysRevSTAB.10.074001 PACS numbers: 29.20.−c

I. INTRODUCTION

Global and local resonance terms were measured in the Super Proton Synchrotron (SPS) and the Relativistic Heavy Ion Collider (RHIC) [1,2] from the Fourier spectrum of turn-by-turn data. The possibility of extending this technique to measure magnet strengths was proposed in [2,3] but could not be applied in the respective accelerators due to technical reasons.

The SPS, equipped with strong sextupoles, is an ideal test-bench to prove the feasibility of magnet strengths measurement. We have used existing beam position monitor (BPM) data acquired in [4]. During this experiment the beam motion was excited by a single kick in the presence of seven strong sextupoles. The existing data have been now reanalyzed using an independent software application [5]. The newly computed resonance driving terms are in agreement with those obtained in [4]. For the first time, the measurement of the strengths of these seven sextupoles using resonance terms is presented here.

This technique can be particularly useful in the commissioning period of an accelerator in order to find magnets with wrong strengths or polarities as well as magnets with large magnetic errors.

In Sec. II the normal form formalism [6,7] is briefly introduced. The scope of this section is threefold. First, it provides the basic ingredients (although already derived in [8]) necessary for the comprehension of the new formulas. Second, it shows how to compute the Hamiltonian coefficients h_{jklm} directly from the magnet strengths, rather than from the harmonic analysis of particle tracking data. Third, as the sign in some exponential terms depends on the choice of the complex Courant-Snyder coordinates $(q \pm ip_q)$, we aim to collect all the fundamental relations making use of a consistent nomenclature. In Sec. III the new formula that allows the computation of magnet strengths from BPM data is presented. The experimental results are presented in Sec. IV, together with a brief description of the new software application developed for the analysis of the BPM data.

II. THEORETICAL BACKGROUND

A. Hamiltonian coefficients and magnet strength

The Hamiltonian describing the particle motion at a generic location of the accelerator b is given by the following expression:

$$H(b) = \sum_{jklm} h^{(b)}_{jklm} (2J_x)^{(j+k)/2} (2J_y)^{(l+m)/2} \times e^{i[(j-k)(\phi_x+\phi_{x,0})+(l-m)(\phi_y+\phi_{y,0})]}, \quad (1)$$

where J_q and ϕ_q are the action phase variables, $\phi_{q,0}$ are the initial phases, and $h^{(b)}_{jklm}$ are the Hamiltonian terms of order $j + k + l + m = n$. These Hamiltonian terms are given by a summation over the magnetic elements of the accelerator in the following form:

$$h^{(b)}_{jklm} = \sum_w h_{w,jklm} e^{i[(j-k)\Delta\phi^b_{w,x}+(l-m)\Delta\phi^b_{w,y}]}, \quad (2)$$

where $\Delta\phi^b_{w,q}$ are the phase advances of the magnet number w with respect to the location b. The coefficients $h_{w,jklm}$ are real and proportional to the multipole strengths via (see Appendix A for the derivation)

$$h_{w,jklm} = -\frac{[K_{w,n-1}\Omega(l+m) + iJ_{w,n-1}\Omega(l+m+1)]}{j!\quad k!\quad l!\quad m!\quad 2^{j+k+l+m}} \times i^{l+m}(\beta_{w,x})^{(j+k)/2}(\beta_{w,y})^{(l+m)/2},$$
$$\Omega(p) = 1 \text{ if } p \text{ is even}, \qquad \Omega(p) = 0 \text{ if } p \text{ is odd}. \quad (3)$$

$\Omega(i)$ is introduced to select either the normal or the skew multipoles. According to the above relation, the dimensions of $h_{w,jklm}$ are $m^{1-[(j+k+l+m)/2]}$. From the measurement of $h_{w,jklm}$ the magnetic strengths can be directly inferred using the betatron functions.

B. Normal form, resonance driving terms, and BPM spectrum

The Hamiltonian H defined in Eq. (1) depends on both the actions J_q and the phases ϕ_q. Nonresonant

normal form coordinates can be introduced to obtain a Hamiltonian that depends only on the action variables $\mathsf{H}(I_x, I_y)$. This transformation is performed by introducing a function F, defined as

$$F(b) = \sum_{jklm} f^{(b)}_{jklm} (2I_x)^{(j+k)/2} (2I_y)^{(l+m)/2} \times e^{i[(j-k)(\psi_x+\psi_{x,0})+(l-m)(\psi_y+\psi_{y,0})]}, \quad (4)$$

where I_q, ψ_q, and $\psi_{q,0}$ are the new actions, phases, and arbitrary initial conditions, respectively. It can be shown [9] that the terms $f^{(b)}_{jklm}$ at a certain location b, in the first-order approximation, are related to the Hamiltonian coefficients $h_{w,jklm}$ via

$$f^{(b)}_{jklm} = \frac{\sum_w h_{w,jklm} e^{i[(j-k)\Delta\phi^b_{w,x}+(l-m)\Delta\phi^b_{w,y}]}}{1 - e^{2\pi i[(j-k)Q_x+(l-m)Q_y]}}, \quad (5)$$

where Q_x and Q_y are the betatron tunes. $f^{(b)}_{jklm}$ (at any location) diverge when a resonance occurs, i.e. when

$$(j-k)Q_x + (l-m)Q_y = p \qquad p \in \mathbf{N}. \quad (6)$$

For this reason f_{jklm} are called resonance driving terms (RDT). The first-order approximation implicit in Eq. (5) is enough as long as we want to measure the magnet strengths of quadrupoles and sextupoles. In [8] the complex Courant-Snyder variable, defined as $h_{x,-} = \hat{x} - i\hat{p}_x$, at turn N and location b is related to the resonance driving terms as

$$h_{x,-}(b,N) = \sqrt{2I_x} e^{i(2\pi\nu_x N+\psi_{b,x,0})} - 2i\sum_{jklm} j f^{(b)}_{jklm} (2I_x)^{(j+k-1)/2} (2I_y)^{(l+m)/2} \times e^{i[(1-j+k)(2\pi\nu_x N+\psi_{b,x,0})+(m-l)(2\pi\nu_y N+\psi_{b,y,0})]}, \quad (7)$$

and, equivalently for the vertical plane,

$$h_{y,-}(b,N) = \sqrt{2I_y} e^{i(2\pi\nu_y N+\psi_{b,y,0})} - 2i\sum_{jklm} l f^{(b)}_{jklm} (2I_x)^{(j+k)/2} (2I_y)^{(l+m-1)/2} \times e^{i[(k-j)(2\pi\nu_x N+\psi_{b,x,0})+(1-l+m)(2\pi\nu_y N+\psi_{b,y,0})]}. \quad (8)$$

Note that neither $h_{x,-}$ nor $h_{y,-}$ are canonical coordinates. This however does not influence the derivation of our final results, since all the observables are eventually related to the canonical coordinates $\hat{x}, \hat{p}_x$ $(\hat{y}, \hat{p}_y)$. For a detailed analysis of the effect of the nonsymplectic transformation, see [6]. The nonlinear tunes $\nu_{x,y}$ appear in the above expression instead of $Q_{x,y}$ since this approach takes into account possible amplitude dependent detuning. The first term in the right-hand side of Eqs. (7) and (8) are called *fundamental* or *tune* lines. The *secondary* lines contained in the summation are generated by all the magnetic perturbations and are proportional to the RDTs. The amplitude and phase of the *secondary* lines in the horizontal spectrum are given by

$$H(1-j+k, l-m) = 2j|f^{(b)}_{jklm}|(2I_x)^{(j+k-1)/2}(2I_y)^{(l+m)/2}, \quad (9)$$

$$\phi_{(1-j+k,l-m)} = \phi^{f^{(b)}_{jklm}} + (1-j+k)\psi_{b,x,0} + (m-l)\psi_{b,y,0} - \frac{\pi}{2}, \quad (10)$$

where $\phi^{f^{(b)}_{jklm}}$ denotes the phase of the RDT f_{jklm}, while $H(p,q)$ and $\phi_{(p,q)}$ stand for the amplitude and phase of the spectral line with frequency $p\nu_x + q\nu_y$ in the horizontal spectrum. Equivalently for the vertical plane,

$$V(k-j, 1+m-l) = 2l|f^{(b)}_{jklm}|(2I_x)^{(j+k)/2}(2I_y)^{(l+m-1)/2}, \quad (11)$$

$$\phi_{(k-j,1+m-l)} = \phi^{f^{(b)}_{jklm}} + (k-j)\psi_{b,x,0} + (1-l+m)\psi_{b,y,0} - \frac{\pi}{2}. \quad (12)$$

The horizontal and vertical tune lines are represented by $H(1,0)$ and $V(0,1)$, respectively. Their amplitudes and phases are

$$H(1,0) = \sqrt{2I_x}, \qquad \phi_{H(1,0)} = \psi_{b,x,0}, \quad (13)$$

$$V(0,1) = \sqrt{2I_y}, \qquad \phi_{V(0,1)} = \psi_{b,y,0}. \quad (14)$$

Note that from Eqs. (6)–(8), the spectral lines $H(1-j+k, l-m)$ and $V(k-j, 1-m+l)$ appear only if $j \neq 0$ and $l \neq 0$, respectively. In Appendix B the correspondences between excited spectral lines and RDTs are listed. Note that the analogous classification concerning the vertical plane has been rectified in the updated version of Ref. [8].

III. MAGNET STRENGTHS FROM RDT VARIATION ALONG THE RING

The difference of the resonance driving terms at two observation locations (BPMs) of the ring, w and $w-1$, depends only on the multipoles placed between these two locations, exactly,

$$\hat{h}_{w,jklm} = f^{(w)}_{jklm} e^{-i[(j-k)\Delta\phi_x^{w,w-1}+(l-m)\Delta\phi_y^{w,w-1}]} - f^{(w-1)}_{jklm}, \quad (15)$$

where $\Delta\phi_q^{w,w-1}$ are the phase advances between the two locations and $f^{(w)}_{jklm}$ is the RDT measured at the BPM number w. An illustrative proof of this relation is given in Appendix C. The left-hand side (lhs) of the above equation is therefore an observable given by

$$\hat{h}_{w,jklm} = \sum_{\tau} h_{\tau,jklm} e^{i[(j-k)\Delta\phi_{\tau,x}^{w-1} + (l-m)\Delta\phi_{\tau,y}^{w-1}]}. \quad (16)$$

The sum runs over all the multipoles between the BPMs number $(w-1)$ and w, while $\Delta\phi_{\tau,q}^{w-1}$ are the phase advances between those multipoles and the BPM number $(w-1)$ (see Fig. 6). $h_{\tau,jklm}$ are the Hamiltonian coefficients defined in Eq. (3). Equation (15) reveals the most important feature of this approach: *the amplitudes of the RDT at two BPMs change only if there are multipoles in between*. Vice versa from the difference between the two RDTs a total strength of the multipoles in between $\hat{h}_{w,jklm}$ is inferred.

In general, it is not possible to derive directly the strengths K and J from $\hat{h}_{w,jklm}$. Nevertheless, in the case that there is only one multipole in between two consecutive BPMs, Eq. (15) simplifies to

$$h_{w,jklm} e^{-i[(j-k)\Delta\phi_x^w + (l-m)\Delta\phi_y^w]} = f_{jklm}^{(w)} e^{-i[(j-k)\Delta\phi_x^{w,w-1} + (l-m)\Delta\phi_y^{w,w-1}]} - f^{(w-1)}. \quad (17)$$

If the betatron phase and the beta functions at the multipole are known, using Eqs. (3) and (17), the strengths $K_{w,n-1}$ and $J_{w,n-1}$ can be inferred.

IV. MAGNET STRENGTH MEASUREMENT FROM SPS DATA

During 2002 a measurement campaign aimed to measure the RDTs was carried out in the SPS at CERN [1,4]. Seven strong sextupoles were connected to introduce large nonlinearities. Their locations and the model parameters are listed in Table I.

Other 108 sextupoles used for the chromaticity correction where also powered. These sextupoles are grouped in four families, whose parameters are listed in Table II.

The new software application *bpm2rdt* has been developed for the analysis of BPM data and is available with documentation [5]. Despite the complex formalism, the input consists only of the number of turns to analyze, the tunes $Q_{x,y}$, and of two external files with the BPM turn-by-turn data and the lattice model (magnet strengths and Twiss parameters), respectively. While the first file is used for the analysis of the experimental data, the second is used to compute all the observables predicted by the model. Note that in general the Twiss parameters at the locations of the multipoles cannot be extracted directly from the BPM data. The code first constructs the observables $h_{q,-}(N)$ at each BPM. Then it performs the fast-Fourier-transform (FFT) of these variables, finds automatically the peaks of the Fourier spectra, and calculates the corresponding RDTs f_{jklm}, the strengths $\hat{h}_{jklm}$, and the local terms χ_{jklm} introduced in [2]. All these observables are printed out together with the prediction from the model for a direct comparison.

TABLE I. Parameters of the seven strong sextupoles.

Name	Location [m]	K_2 [m^{-1}]	β_x [m]	h_{3000} [$m^{-1/2}$]
LSE.1060	766.2	0.446 29	96.335	8.7913
LSE.1240	1342.2	0.446 29	92.238	8.2365
LSE.2060	1918.2	0.446 29	100.542	9.3734
LSE.2240	3646.1	−0.446 29	100.210	−9.3271
LSE.4060	4222.0	−0.446 29	90.488	−8.0032
LSEN.424	4798.0	−0.446 29	97.020	−8.8852
LSE.5240	5373.9	−0.446 29	94.413	−8.5300

TABLE II. Parameters of the 108 chromaticity sextupoles.

Family name	Number	K_2 [m^{-1}]	β_x [m]
LSFA/C	36	−0.022 45	∼100
LSFB	18	−0.044 96	∼100
LSDA	18	0.084 17	∼22
LSDB	36	0.066 41	∼22

Note that the relations listed in Table IV are derived assuming turn-by-turn oscillations without decoherence and properly calibrated BPMs. To take into account the decoherence of the SPS data, the measured f_{3000} has been multiplied by the *decoherence factor* 2. In Ref. [1] it is indeed proved how the decoherence of the BPM signal reduces the amplitude of each secondary spectral line by a factor that depends on both the excited resonance and the amplitude detuning ν'. The decoherence factor of a generic horizontal spectral line $(1-j+k, m-l)$ is defined as $|1-j+k+(m-l)\nu'_{yx}/\nu'_{xx}|$ and represents the reduction factor when compared to the single-particle case (our model).

In Fig. 1 the measured f_{3000} is plotted around the ring together with the prediction from the model. Model and measurement are in good agreement as in [4]. However, the

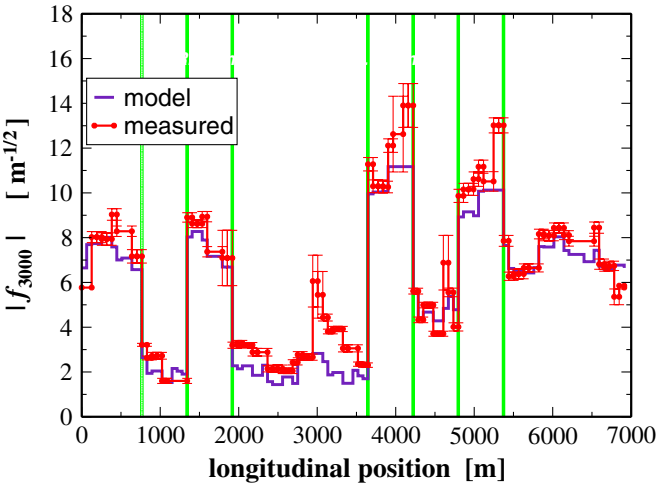

FIG. 1. (Color) RDT f_{3000} along the ring. The vertical lines indicate the location of the seven extraction sextupoles. Error bars correspond to 1σ. Only the values from BPMs providing error bars smaller than 20% are shown.

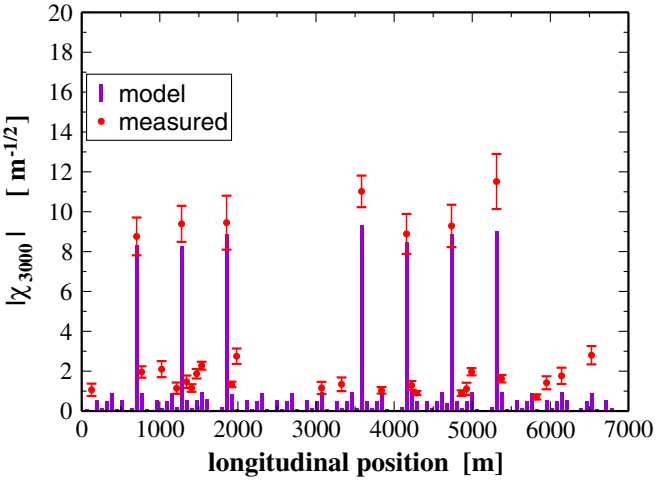

FIG. 2. (Color) Measured and expected absolute value of χ_{3000}. Error bars correspond to 3σ. Only the values providing error bars smaller than 20% are shown.

measured f_{3000} shows small jumps at locations where they were not expected. This is due to an intrinsic error in constructing the complex variable $h_{q,-} = q - ip_q$. Indeed to compute the momentum p_q at a given BPM, the position (in normalized coordinates) measured at the next BPM is used [10]:

$$\hat{p}_{i,q} = (\hat{q}_{i+1} - \hat{q}_i \cos\Delta\phi_q)/\sin\Delta\phi_q, \qquad (18)$$

where $\Delta\phi_q$ is the phase advance between the two BPMs. This formula however applies only in the absence of nonlinearities or coupling sources between the two monitors. If this condition is not satisfied because the computation of p_q contains an intrinsic error, whose estimation is given in [2], that may reveal in artificial jumps.

To avoid this problem, a new observable was defined in [2] using data from three consecutive BPM. This new signal does not require any momentum reconstruction and the local terms χ_{jklm} that are computed from its spectrum have the same physical meaning as the Hamiltonian terms $\hat{h}_{jklm}$, although the measurement of χ_{jklm} is more accurate. In Fig. 2 χ_{3000} measured from the SPS data is plotted and, as expected, no term is visible in the region with the unexpected jump of f_{3000}. Despite the fact that χ_{jklm} is an observable more robust than $\hat{h}_{jklm}$, it exists an additional difference that needs to be stressed for a correct interpretation of the measurement, χ_{jklm} being defined as

$$\chi_{jklm} = \sum_q e^{i[(1-j+k)\phi_{xq}+(m-l)\phi_{yq}]} SEN(\phi_{xq}) h_{q,jklm}. \qquad (19)$$

The above summation extends over the multipoles in between the three BPMs, $h_{q,jklm}$ are the Hamiltonian coefficients defined in Eq. (3) of the multipole number q, whose phase advances with respect to the first BPM are ϕ_{xq} and ϕ_{yq}. $SEN(\phi_{xq})$ is defined as

$$\begin{cases} \sin\phi_{xq}\sqrt{1+\tan^2\delta_{x,1}}, & \text{if } \phi_{xq} < \Delta\phi_{x,1} \\ \sin(\phi_{xq} - \delta_{x,1} - \delta_{x,2})\sqrt{1+\tan^2\delta_{x,2}}, & \text{if } \phi_{xq} > \Delta\phi_{x,1}, \end{cases}$$

where $\delta_{x,1} = \Delta\phi_{x,1} - \pi/2$, and $\delta_{x,2} = \Delta\phi_{x,2} - \pi/2$. $\Delta\phi_{x,1}$ and $\Delta\phi_{x,2}$ are the phase advances between the first and the second BPM and between the second and the third, respectively. If the BPMs are 90 degrees apart (and this is the case for the SPS BPMs), χ_{jklm} and $\hat{h}_{jklm}$ are equivalent, while the first one diverges if the distance is close to 180 degrees. Hence, when measuring large χ_{jklm}, one has to

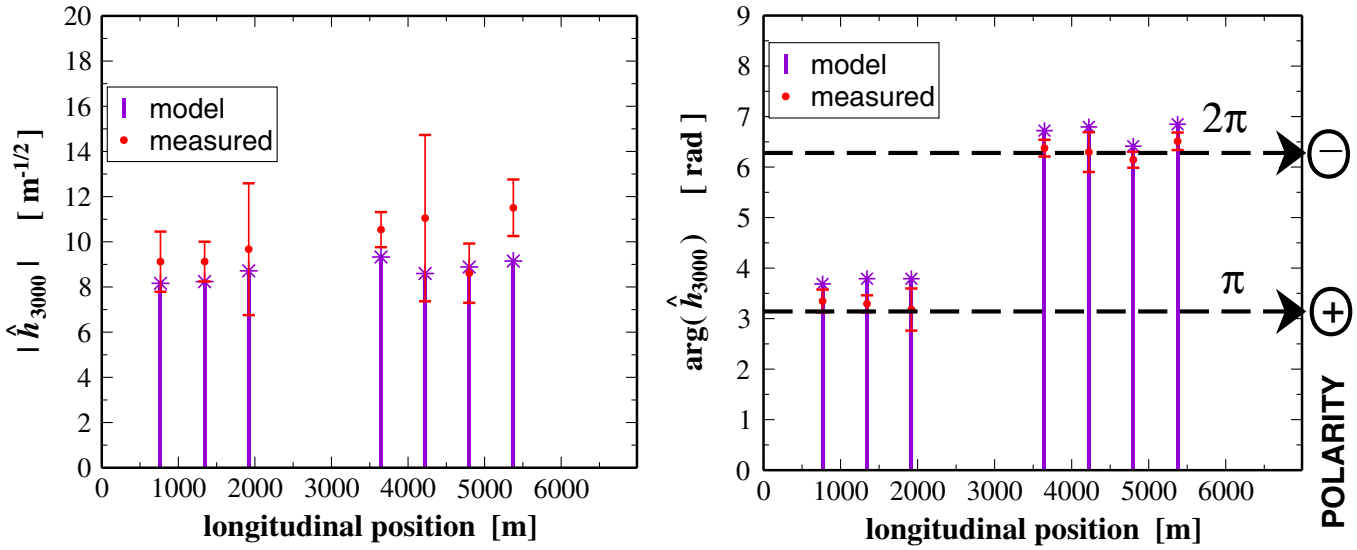

FIG. 3. (Color) Measured and expected absolute value and phase of $\hat{h}_{3000}$ corresponding to the seven excited extraction sextupoles. Error bars correspond to 3σ.

look at the BPM phase advances before extrapolating any information on the local sources of nonlinearities.

Because of the BPM distribution, the sextupoles LSE.1240, LSE.2240, and LSEN.424 (see Table I) fulfill the condition of being the only source of nonlinearities between the two adjacent BPMs. The other four extraction sextupoles have at least another chromaticity sextupole in between the two adjacent BPMs. However, the extraction sextupoles are much stronger than the chromaticity sextupoles and as first approximation the chromaticity sextupoles might be neglected.

In Fig. 3 the measured $\hat{h}_{3000}$ are plotted together with the predictions from the model. The agreement for $|\hat{h}_{3000}|$ varies from 3% (LSEN.424) to 28% (LSE.4060). Error in the phases is of about 10%, confirming the correct setting of the polarities. Because of the lattice configuration of the SPS, the phases of $\hat{h}_{3000}$ provide a direct measurement of their polarities as shown in the figure.

V. CONCLUSION

A beam based method to measure the magnet strengths and polarities has been presented. The method is based on the harmonic analysis of multi-BPM turn-by-turn data of a transversally kicked beam. Both the new algorithm and the software application *bpm2rdt* have been successfully tested by using existing SPS data.

ACKNOWLEDGMENTS

The authors thank G. Franchetti (GSI), A. Bazzani (University of Bologna), P. Moritz (GSI), and T. Beier (GSI) for having contributed to the software development. We are also thankful to G. Arduini for reading the manuscript and providing valuable comments. One of the authors (A. F.) acknowledges this work was partially support by GSI, Darmstadt.

APPENDIX A: FROM MAGNET STRENGTH TO HAMILTONIAN COEFFICIENTS

In this Appendix we derive Eq. (3), starting from the Hamiltonian describing a multipole of order n:

$$H^{(n)} = -\mathrm{Re}\left\{\frac{(K_{n-1} + iJ_{n-1})}{n!}(x + iy)^n\right\}. \tag{A1}$$

According to the binomial theorem, the Hamiltonian can be expanded in series as

$$H^{(n)} = -\mathrm{Re}\left\{\sum_{p=0}^{n}\frac{(K_{n-1} + iJ_{n-1})}{(n-p)!p!}x^p(iy)^{n-p}\right\}. \tag{A2}$$

Defining $p = j + k$ and $n - p = l + m$ (note that $n = j + k + l + m$), the above equation reads

$$H^{(n)} = -\mathrm{Re}\left\{\sum_{\substack{j+k=0\\ l+m=n-j-k}}^{n}\frac{(K_{n-1} + iJ_{n-1})}{(l+m)!(j+k)!}x^{j+k}(iy)^{l+m}\right\}. \tag{A3}$$

Introducing the complex Courant-Snyder coordinates $q = \frac{\sqrt{\beta_q}}{2}(h_{q,-} + h_{q,+})$, where $h_{q,\pm} = \sqrt{2J_q}e^{\mp i(\phi_q+\phi_{q,0})}$, and q stands for x or y, we obtain

$$H^{(n)} = -\mathrm{Re}\left\{\sum_{\substack{j+k\\ l+m}}^{n}\frac{(K_{n-1} + iJ_{n-1})}{(l+m)!(j+k)!}\beta_x^{(j+k)/2}\beta_y^{(l+m)/2} \times\frac{i^{l+m}}{2^{j+k+l+m}}(h_{x,-} + h_{x,+})^{j+k}(h_{y,-} + h_{y,+})^{l+m}\right\}. \tag{A4}$$

The binomial theorem can be invoked again to expand $(h_{q,-} + h_{q,+})$

$$H^{(n)} = -\mathrm{Re}\left\{\sum_{\substack{j+k\\ l+m}}^{n}\frac{(K_{n-1} + iJ_{n-1})}{(l+m)!(j+k)!}\beta_x^{(j+k)/2}\beta_y^{(l+m)/2} \times\frac{i^{l+m}}{2^{j+k+l+m}}\sum_{s=0}^{j+k}\sum_{t=0}^{l+m}\frac{(j+k)!(l+m)!}{(j+k-s)!(l+m-t)!s!t!} \times h_{x,-}^{s}h_{x,+}^{j+k-s}h_{y,-}^{t}h_{y,+}^{l+m-t}\right\}. \tag{A5}$$

Renaming the indexes $s \longrightarrow j$ and $t \longrightarrow l$ and simplifying the factorials, the Hamiltonian reads

$$H^{(n)} = -\mathrm{Re}\left\{\sum_{j,k,l,m=0}^{n=j+k+l+m}\frac{(K_{n-1} + iJ_{n-1})}{j!k!l!m!2^{j+k+l+m}} \times\beta_x^{(j+k)/2}\beta_y^{(l+m)/2}i^{l+m}h_{x,-}^{j}h_{x,+}^{k}h_{y,-}^{l}h_{y,+}^{m}\right\}. \tag{A6}$$

It can be easily shown that the real part of the sum selects the normal terms K_{n-1} if the power of y (i.e. $l + m$) is even, whereas the skew terms J_{n-1} are selected when $l + m$ is odd (See Table III). This selection can be expressed introducing a function Ω such that

$$\Omega(p) = 1 \text{ if } p \text{ is even}, \quad \Omega(p) = 0 \text{ if } p \text{ is odd}, \tag{A7}$$

which can be included in the Hamiltonian according to

TABLE III. Selection of index relative to the main corrector magnets.

Multipole kind	n	Potential term	Index relations
Normal quadrupole x	2	x^2	$j+k=2 \quad m+l=0$
Normal quadrupole y	2	y^2	$j+k=0 \quad m+l=2$
Skew quadrupole	2	xy	$j+k=1 \quad m+l=1$
Normal sextupole 1	3	x^3	$j+k=3 \quad m+l=0$
Normal sextupole 2	3	xy^2	$j+k=1 \quad m+l=2$
Skew sextupole 1	3	y^3	$j+k=0 \quad m+l=3$
Skew sextupole 2	3	x^2y	$j+k=2 \quad m+l=1$

$$H^{(n)} = \sum_{j,k,l,m=0}^{n=j+k+l+m} - \frac{[K_{n-1}\Omega(l+m) + iJ_{n-1}\Omega(l+m+1)]}{j!k!l!m!2^{j+k+l+m}} \times \beta_x^{(j+k)/2}\beta_y^{(l+m)/2} i^{l+m} h^j_{x,-} h^k_{x,+} h^l_{y,-} h^m_{y,+}. \quad \text{(A8)}$$

From the above relation, one derives Eq. (3).

APPENDIX B: RESONANCE CLASSIFICATION AND NOMENCLATURE

The starting points for a complete classification (up to the first order) of RDT, spectral lines, and resonances are the following relations:

$$(j-k)Q_x + (l-m)Q_y = p \in \mathbf{N} \quad \text{excited resonance,} \quad \text{(B1)}$$

$$H(1-j+k, m-l) \quad \text{horiz. line, if } j \neq 0, \quad \text{(B2)}$$

$$V(k-j, 1-l+m) \quad \text{vert. line, if } l \neq 0. \quad \text{(B3)}$$

The generic potential term $x^s y^q$ selects the index $j+k=s$ and $m+l=q$, as shown in Eq. (A2). The relations between the RDTs and the excited spectral lines are given in Table IV, where the line amplitudes $|a_{jklm}|$ and the phases ϕ^a_{jklm} are derived from Eqs. (9)–(12). In Fig. 4 some typical BPM spectra obtained by single-particle tracking are also shown.

Table V shows how to compute the RDT from the spectral lines, i.e., how to remove the dependences from $I_{x,y}$ and $\phi_{x,y,0}$, assuming that the BPMs are properly calibrated.

APPENDIX C: CALCULATION OF THE MAGNET STRENGTH FROM THE RDTS

In this Appendix we provide an illustrative proof of Eq. (15). First we consider the case with only one magnet between two consecutive BPMs (see Fig. 5).

It is convenient to define some quantities as follows:

$$\mathsf{B}_b = i[(j-k)\phi^{\mathrm{BPM}}_{b,x} + (l-m)\phi^{\mathrm{BPM}}_{b,y}], \quad \text{(C1)}$$

$$\mathsf{W}_w = i[(j-k)\phi^{M}_{w,x} + (l-m)\phi^{M}_{w,y}], \quad \text{(C2)}$$

$$\mathsf{Q} = 2\pi i[(j-k)Q_x + (l-m)Q_y], \quad \text{(C3)}$$

$$h^{(b)}_{jklm} = \sum_{w \le b} h_{w,jklm} e^{\mathsf{B}_b - \mathsf{W}_w} + \sum_{w>b} h_{w,jklm} e^{\mathsf{B}_b - \mathsf{W}_w + \mathsf{Q}}. \quad \text{(C4)}$$

ϕ^M_w and $\phi^{\mathrm{BPM}}_{b,q}$ are the betatron phases of the magnet number w and the BPM number b, respectively, both calculated with respect to a starting point. Each time $b < w$ a factor Q must be added to take into account the *crossing* of this point. With the above nomenclature, Eq. (5) reads

$$f^{(b)}_{jklm} = \frac{h^{(b)}_{jklm}}{1 - e^{\mathsf{Q}}}. \quad \text{(C5)}$$

$h_{w,jklm}$ are calculated inverting the linear system (C5). For the sake of clarity, we show a case with $W=3$ (the generalization to any number is straightforward) and omit the subscript $jklm$,

$$h^{(1)} = e^{\mathsf{B}_1 - \mathsf{W}_1} h_1 + e^{\mathsf{B}_1 - \mathsf{W}_2 + \mathsf{Q}} h_2 + e^{\mathsf{B}_1 - \mathsf{W}_3 + \mathsf{Q}} h_3,$$
$$h^{(2)} = e^{\mathsf{B}_2 - \mathsf{W}_1} h_1 + e^{\mathsf{B}_2 - \mathsf{W}_2} h_2 + e^{\mathsf{B}_2 - \mathsf{W}_3 + \mathsf{Q}} h_3,$$
$$h^{(3)} = e^{\mathsf{B}_3 - \mathsf{W}_1} h_1 + e^{\mathsf{B}_3 - \mathsf{W}_2} h_2 + e^{\mathsf{B}_3 - \mathsf{W}_3} h_3.$$

In the matrix notation the system reads $\vec{H} = \mathbf{A}\vec{h}$,

$$\begin{pmatrix} h^{(1)} \\ h^{(2)} \\ h^{(3)} \end{pmatrix} = \begin{pmatrix} e^{\mathsf{B}_1 - \mathsf{W}_1} & e^{\mathsf{B}_1 - \mathsf{W}_2 + \mathsf{Q}} & e^{\mathsf{B}_1 - \mathsf{W}_3 + \mathsf{Q}} \\ e^{\mathsf{B}_2 - \mathsf{W}_1} & e^{\mathsf{B}_2 - \mathsf{W}_2} & e^{\mathsf{B}_2 - \mathsf{W}_3 + \mathsf{Q}} \\ e^{\mathsf{B}_3 - \mathsf{W}_1} & e^{\mathsf{B}_3 - \mathsf{W}_2} & e^{\mathsf{B}_3 - \mathsf{W}_3} \end{pmatrix} \begin{pmatrix} h_1 \\ h_2 \\ h_3 \end{pmatrix}. \quad \text{(C6)}$$

$\mathbf{A}$ can be factorized as $\mathbf{A} = \mathbf{A}_1\mathbf{A}_2$,

$$\mathbf{A} = \begin{pmatrix} e^{\mathsf{B}_1} & 0 & 0 \\ 0 & e^{\mathsf{B}_2} & 0 \\ 0 & 0 & e^{\mathsf{B}_3} \end{pmatrix} \begin{pmatrix} e^{-\mathsf{W}_1} & e^{-\mathsf{W}_2 + \mathsf{Q}} & e^{-\mathsf{W}_3 + \mathsf{Q}} \\ e^{-\mathsf{W}_1} & e^{-\mathsf{W}_2} & e^{-\mathsf{W}_3 + \mathsf{Q}} \\ e^{-\mathsf{W}_1} & e^{-\mathsf{W}_2} & e^{-\mathsf{W}_3} \end{pmatrix}.$$

$\mathbf{A}_2$ is inverted according to $\mathbf{A}_2 = (\mathbf{A}_3\mathbf{A}_4)^{-1}$,

$$\mathbf{A}_2 = -\left[\begin{pmatrix} e^{\mathsf{W}_1} & 0 & -e^{\mathsf{W}_1 + \mathsf{Q}} \\ -e^{\mathsf{W}_2} & e^{\mathsf{W}_2} & 0 \\ 0 & -e^{\mathsf{W}_3} & e^{\mathsf{W}_3} \end{pmatrix} \begin{pmatrix} \frac{1}{1-e^{\mathsf{Q}}} & 0 & 0 \\ 0 & \frac{1}{1-e^{\mathsf{Q}}} & 0 \\ 0 & 0 & \frac{1}{1-e^{\mathsf{Q}}} \end{pmatrix} \right]^{-1}.$$

TABLE IV. List of spectral lines driven by resonances and corresponding RDTs.

Quadrupole term $\propto x^2, y^2$						
n	$jklm$	Resonance	H-line	V-line	$\lvert a_{jklm}\rvert$	ϕ^a_{jklm}
2	1100	(2, 0)	(1, 0)		$(2I_x)^{1/2}$	$\psi_{x,0}$
2	2000	(2, 0)	(−1, 0)		$4\lvert f_{2000}\rvert(2I_x)^{1/2}$	$\phi^f_{2000} - \psi_{x,0}$
2	0011	(0, 2)		(0, 1)	$(2I_y)^{1/2}$	$\psi_{y,0}$
2	0020	(0, 2)		(0, −1)	$4\lvert f_{0020}\rvert(2I_y)^{1/2}$	$\phi^f_{0020} - \psi_{y,0}$
Skew quadrupole term $\propto xy$						
n	$jklm$	Resonance	H-line	V-line	$\lvert a_{jklm}\rvert$	ϕ^a_{jklm}
2	0110	(1, −1)		(1, 0)	$2\lvert f_{0110}\rvert(2I_x)^{1/2}$	$\phi^f_{0110} + \psi_{x,0} - \frac{\pi}{2}$
2	1001	(1, −1)	(0, 1)		$2\lvert f_{1001}\rvert(2I_y)^{1/2}$	$\phi^f_{1001} + \psi_{y,0} - \frac{\pi}{2}$
2	1010	(1, 1)	(0, −1)	(−1, 0)	H: $2\lvert f_{1010}\rvert(2I_y)^{1/2}$	H: $\phi^f_{1010} - \psi_{y,0} - \frac{\pi}{2}$
					V: $2\lvert f_{1010}\rvert(2I_x)^{1/2}$	V: $\phi^f_{1010} - \psi_{x,0} - \frac{\pi}{2}$
Normal sextupole term $\propto x^3$						
n	$jklm$	Resonance	H-line	V-line	$\lvert a_{jklm}\rvert$	ϕ^a_{jklm}
3	1200	(1,0)	(2, 0)		$2\lvert f_{1200}\rvert(2I_x)$	$\phi^f_{1200} + 2\psi_{x,0} - \frac{\pi}{2}$
3	2100	(1,0)	(0, 0)		$4\lvert f_{2100}\rvert(2I_x)$	$\phi^f_{2100} - \frac{\pi}{2}$
3	3000	(3,0)	(−2, 0)		$6\lvert f_{3000}\rvert(2I_x)$	$\phi^f_{3000} - 2\psi_{x,0} - \frac{\pi}{2}$
Normal sextupole term $\propto xy^2$						
n	$jklm$	Resonance	H-line	V-line	$\lvert a_{jklm}\rvert$	ϕ^a_{jklm}
3	0111	(1,0)		(1, 1)	$2\lvert f_{0111}\rvert(2I_x2I_y)^{1/2}$	$\phi^f_{0111} + \psi_{x,0} + \psi_{y,0} - \frac{\pi}{2}$
3	0120	(1, −2)		(1, −1)	$4\lvert f_{0120}\rvert(2I_x2I_y)^{1/2}$	$\phi^f_{0120} + \psi_{x,0} - \psi_{y,0} - \frac{\pi}{2}$
3	1002	(1, −2)	(0, 2)		$2\lvert f_{1002}\rvert(2I_y)$	$\phi^f_{1002} + 2\psi_{y,0} - \frac{\pi}{2}$
3	1011	(1,0)	(0, 0)	(−1, 1)	H: $2\lvert f_{1011}\rvert(2I_y)$	H: $\phi^f_{1011} - \frac{\pi}{2}$
					V: $2\lvert f_{1011}\rvert(2I_x2I_y)^{1/2}$	V: $\phi^f_{1011} - \psi_{x,0} + \psi_{y,0} - \frac{\pi}{2}$
3	1020	(1,2)	(0, −2)	−(1, 1)	H: $2\lvert f_{1020}\rvert(2I_y)$	H: $\phi^f_{1020} - 2\psi_{y,0} - \frac{\pi}{2}$
					V: $4\lvert f_{1020}\rvert(2I_x2I_y)^{1/2}$	V: $\phi^f_{1020} - \psi_{x,0} - \psi_{y,0} - \frac{\pi}{2}$
Skew sextupole term $\propto y^3$						
n	$jklm$	Resonance	H-line	V-line	$\lvert a_{jklm}\rvert$	ϕ^a_{jklm}
3	0012	(0,1)		(0, 2)		
3	0021	(0,1)		(0, 0)	$4\lvert f_{0021}\rvert(2I_y)$	$\phi^f_{0021} - \frac{\pi}{2}$
3	0030	(0,3)		(0, −2)	$6\lvert f_{0030}\rvert(2I_y)$	$\phi^f_{0030} - 2\psi_{y,0} - \frac{\pi}{2}$
Skew sextupole term $\propto x^2y$						
n	$jklm$	Resonance	H-line	V-line	$\lvert a_{jklm}\rvert$	ϕ^a_{jklm}
3	1101	(0,1)	(1, 1)		$2\lvert f_{1101}\rvert(2I_x2I_y)^{1/2}$	$\phi^f_{1101} + \psi_{x,0} + \psi_{y,0} - \frac{\pi}{2}$
3	2001	(2, −1)	(−1, 1)		$4\lvert f_{2001}\rvert(2I_x2I_y)^{1/2}$	$\phi^f_{2001} - \psi_{x,0} + \psi_{y,0} - \frac{\pi}{2}$
3	0210	(2, −1)		(2, 0)	$2\lvert f_{0210}\rvert(2I_x)$	$\phi^f_{0210} + 2\psi_{x,0} - \frac{\pi}{2}$
3	1110	(0,1)	(1, −1)	(0, 0)	H: $2\lvert f_{1110}\rvert(2I_x2I_y)^{1/2}$	H: $\phi^f_{1110} + \psi_{x,0} - \psi_{y,0} - \frac{\pi}{2}$
					V: $2\lvert f_{1110}\rvert(2I_x)$	V: $\phi^f_{1110} - \frac{\pi}{2}$
3	2010	(2,1)	−(1, 1)	(−2, 0)	H: $4\lvert f_{2010}\rvert(2I_x2I_y)^{1/2}$	H: $\phi^f_{2010} - \psi_{x,0} - \psi_{y,0} - \frac{\pi}{2}$
					V: $2\lvert f_{2010}\rvert(2I_x)$	V: $\phi^f_{2010} - 2\psi_{x,0} - \frac{\pi}{2}$

The linear system eventually reads

$$\vec{H} = \mathbf{A}_1(\mathbf{A}_3\mathbf{A}_4)^{-1}\vec{h} \rightarrow \vec{h} = \mathbf{A}_3\mathbf{A}_4\mathbf{A}_1^{-1}\vec{H},$$

providing the solution

$$\begin{pmatrix} h_1 \\ h_2 \\ h_3 \end{pmatrix} = \frac{1}{1-e^{\mathsf{Q}}} \begin{pmatrix} e^{\mathsf{W}_1}(h^{(1)}e^{-\mathsf{B}_1} - h^{(3)}e^{\mathsf{Q}-\mathsf{B}_3}) \\ e^{\mathsf{W}_2}(h^{(2)}e^{-\mathsf{B}_2} - h^{(1)}e^{-\mathsf{B}_1}) \\ e^{\mathsf{W}_3}(h^{(3)}e^{-\mathsf{B}_3} - h^{(2)}e^{-\mathsf{B}_2}) \end{pmatrix}.$$

From Eq. (C5) we obtain

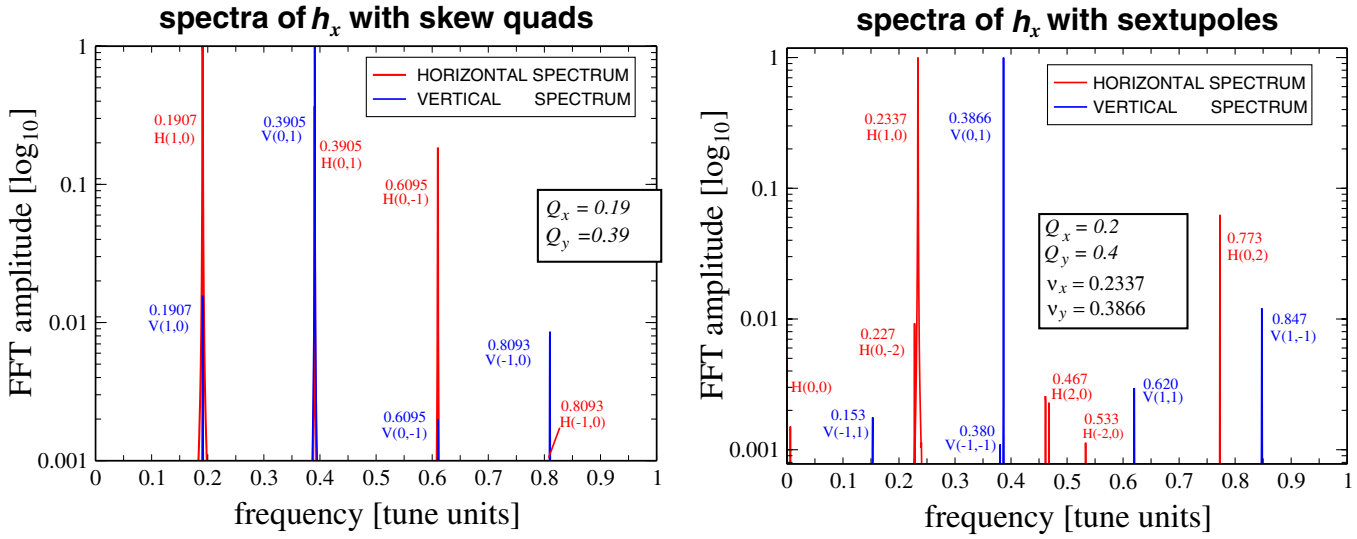

FIG. 4. (Color) Examples of BPM spectra from single-particle tracking simulation with betatron coupling driven by skew quadrupoles (left plot) and nonlinearities driven by normal sextupoles (right plot). Q and ν denote the bare tunes and the nonlinear tunes, respectively.

TABLE V. Formulas to calculate f_{jklm} from the secondary lines assuming properly calibrated BPMs and turn-by-turn oscillations without decoherence.

RDT f_{jklm}	RDT amplitude $\lvert f_{jklm}\rvert$	RDT phase ϕ^f_{jklm}
f_{0110}	$V(1,0)/[2H(1,0)]$	$\phi_{V(1,0)} - \phi_{H(1,0)} + \frac{\pi}{2}$
f_{1001}	$H(0,1)/[2V(0,1)]$	$\phi_{H(0,1)} - \phi_{V(0,1)} + \frac{\pi}{2}$
f^H_{1010}	$H(0,-1)/[2V(0,1)]$	$\phi_{H(0,-1)} + \phi_{V(0,1)} + \frac{\pi}{2}$
f^V_{1010}	$V(-1,0)/[2H(1,0)]$	$\phi_{V(-1,0)} + \phi_{H(1,0)} + \frac{\pi}{2}$
f_{0111}	$V(1,1)/[2H(1,0)V(0,1)]$	$\phi_{V(1,1)} - \phi_{H(1,0)} - \phi_{V(0,1)} + \frac{\pi}{2}$
f_{0120}	$V(1,-1)/[4H(1,0)V(0,1)]$	$\phi_{V(1,-1)} - \phi_{H(1,0)} + \phi_{V(0,1)} + \frac{\pi}{2}$
f_{1002}	$H(0,2)/[2V(0,1)^2]$	$\phi_{H(0,2)} - 2\phi_{V(0,1)} + \frac{\pi}{2}$
f_{1011}	$V(-1,1)/[2H(1,0)V(0,1)]$	$\phi_{V(-1,1)} + \phi_{H(1,0)} - \phi_{V(0,1)} + \frac{\pi}{2}$
f^H_{1020}	$H(0,-2)/[2V(0,1)^2]$	$\phi_{H(0,-2)} + 2\phi_{V(0,1)} + \frac{\pi}{2}$
f^V_{1020}	$V(-,1-1)/[4H(1,0)V(0,1)]$	$\phi_{V(-1,-1)} + \phi_{H(1,0)} + \phi_{V(0,1)} + \frac{\pi}{2}$
f_{1200}	$H(2,0)/[2H(1,0)^2]$	$\phi_{H(2,0)} - 2\phi_{H(1,0)} + \frac{\pi}{2}$
f_{3000}	$H(-2,0)/[6H(1,0)^2]$	$\phi_{H(-2,0)} + 2\phi_{H(1,0)} + \frac{\pi}{2}$
f_{1101}	$H(1,1)/[2H(1,0)V(0,1)]$	$\phi_{H(1,1)} - \phi_{H(1,0)} - \phi_{V(0,1)} + \frac{\pi}{2}$
f_{2001}	$H(-1,1)/[4H(1,0)V(0,1)]$	$\phi_{H(-1,1)} + \phi_{H(1,0)} - \phi_{V(0,1)} + \frac{\pi}{2}$
f_{0210}	$V(2,0)/[2H(1,0)^2]$	$\phi_{V(2,0)} - 2\phi_{H(1,0)} + \frac{\pi}{2}$
f_{1110}	$H(1,-1)/[2H(1,0)V(0,1)]$	$\phi_{H(1,-1)} - \phi_{H(1,0)} + \phi_{V(0,1)} + \frac{\pi}{2}$
f^H_{2010}	$H(-1,-1)/[4H(0,1)V(0,1)]$	$\phi_{H(-1,-1)} + \phi_{H(1,0)} + \phi_{V(0,1)} + \frac{\pi}{2}$
f^V_{2010}	$V(-2,0)/[2H(1,0)^2]$	$\phi_{V(-2,0)} + 2\phi_{H(1,0)} + \frac{\pi}{2}$
f_{0012}	$V(0,2)/[2V(0,1)^2]$	$\phi_{V(0,2)} - 2\phi_{V(0,1)} + \frac{\pi}{2}$
f_{0030}	$V(0,-2)/[6V(0,1)^2]$	$\phi_{V(0,-2)} + 2\phi_{V(0,1)} + \frac{\pi}{2}$

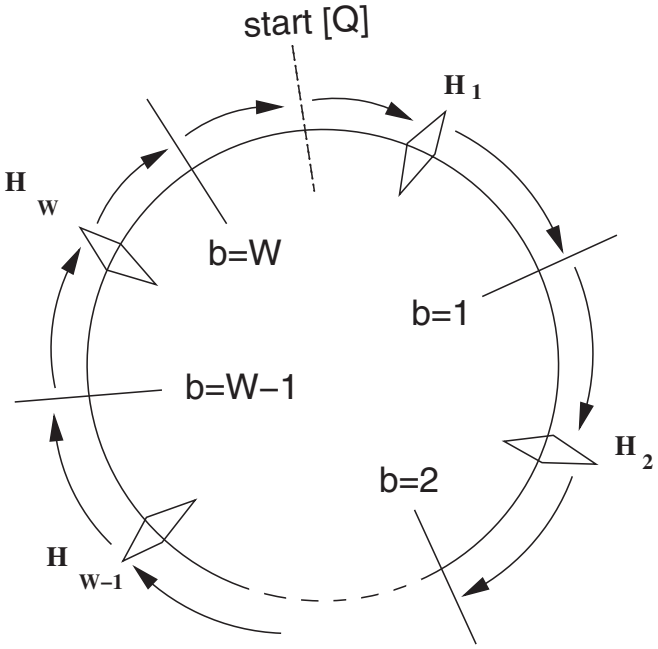

FIG. 5. Schematic view of a ring taking into account the distribution of BPMs and multipoles.

$$\begin{pmatrix} h_1 \\ h_2 \\ h_3 \end{pmatrix} = \begin{pmatrix} e^{\mathsf{W}_1}(f^{(1)}e^{-\mathsf{B}_1} - f^{(3)}e^{\mathsf{Q}-\mathsf{B}_3}) \\ e^{\mathsf{W}_2}(f^{(2)}e^{-\mathsf{B}_2} - f^{(1)}e^{-\mathsf{B}_1}) \\ e^{\mathsf{W}_3}(f^{(3)}e^{-\mathsf{B}_3} - f^{(2)}e^{-\mathsf{B}_2}) \end{pmatrix}. \tag{C7}$$

The general expression for the above equations reads

$$h_w = e^{\mathsf{W}_w}(f^{(w)}e^{-\mathsf{B}_w} - f^{(w-1)}e^{-\mathsf{B}_{w-1}}), \quad \text{for } 2 \le w \le W$$
$$h_1 = e^{\mathsf{W}_1}(f^{(1)}e^{-\mathsf{B}_1} - f^{(W)}e^{\mathsf{Q}-\mathsf{B}_W}). \tag{C8}$$

Reinserting the index $jklm$ and making explicit W_w, B_w, and Q, we obtain

$$h_{w,jklm}e^{-i[(j-k)\Delta\phi_x^{wb}+(l-m)\Delta\phi_y^{wb}]} = f_{jklm}^{(w)}e^{-i[(j-k)\Delta\phi_x^{w,w-1}+(l-m)\Delta\phi_y^{w,w-1}]} - f^{(w-1)}, \tag{C9}$$

where $\Delta\phi_q^{wb}$ are the phase advances between the magnet number w and the BPM number $(w-1)$, whereas $\Delta\phi_q^{w,w-1}$ the phase advances between the two consecutive BPMs.

The most general case with T sources between two consecutive BPMs introduces a modification in the lhs of the above equation, namely, the replacement of the single Hamiltonian coefficient with a sum of all the contributions,

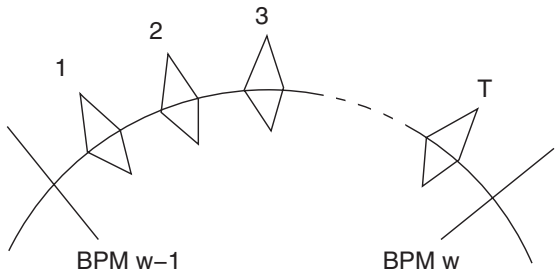

FIG. 6. Schematic view of a section of the ring when several multipoles are placed between two BPMs.

$$h_{w,jklm}e^{-i[(j-k)\Delta\phi_x^{wb}+(l-m)\Delta\phi_y^{wb}]} \rightarrow \hat{h}_{w,jklm}, \tag{C10}$$

where

$$\hat{h}_{w,jklm} = \sum_{\tau=1}^{T} h_{\tau,jklm}e^{i[(j-k)\Delta\phi_{\tau,x}^{w-1}+(l-m)\Delta\phi_{\tau,y}^{w-1}]}. \tag{C11}$$

The sum is over all the T multipoles between the BPMs number $(w-1)$ and w, $\Delta\phi_{\tau,q}^{w-1}$ are the phase advances between those multipoles and the BPM number $(w-1)$ (see Fig. 6).

[1] R. Tomás García, Ph.D. thesis, University of Valencia, Spain, 2003, CERN-THESIS-2003-010.
[2] R. Tomás, M. Bai, R. Calaga, W. Fischer, A. Franchi, and G. Rumolo, Phys. Rev. ST Accel. Beams **8**, 024001 (2005).
[3] A. Franchi, T. Beier, M. Kirk, P. Moritz, G. Rumolo, and R. Tomás, Proceedings of EPAC 2004, Lucerne, p. 1957.
[4] F. Schmidt, M. Hayes, and R. Tomás, the 2003 Particle Accelerator Conference, Portland, Oregon.
[5] A. Franchi, Ph.D. thesis, J. W. Goethe University, Frankfurt am Main, Germany, 2006, GSI DISS 2006-07.
[6] A. Bazzani, E. Todesco, G. Turchetti, and G. Servizi, CERN 94-02, 1994.
[7] M. Berz, É. Forest, and J. Irwin, Part. Accel. **24**, 91 (1989).
[8] R. Bartolini and F. Schmidt, Part. Accel. **59**, 93 (1998).
[9] É. Forest, J. Math. Phys. (N.Y.) **31**, 1133 (1990).
[10] D. D. Caussyn, M. Ball, B. Brabson, J. Collins, S. A. Curtis, V. Derenchuk, D. DuPlantis, G. East, M. Ellison, T. Ellison, D. Friesel, B. Hamilton, W. P. Jones, W. Lamble, S. Y. Lee, D. Li, M. G. Minty, T. Sloan, G. Xu, A. W. Chao, K. Y. Ng, and S. Tepikian, Phys. Rev. A **46**, 7942 (1992).